Eur. Phys. J. A **17**, 415–418 (2003)
DOI 10.1140/epja/i2002-10200-0

THE EUROPEAN PHYSICAL JOURNAL A

Neutron-deuteron scattering in chiral effective field theory

E. Epelbaum[1,a], A. Nogga[2], H. Witała[3], H. Kamada[4], W. Glöckle[1], and U.-G. Meißner[5,6]

[1] Ruhr-Universität Bochum, Institut für Theoretische Physik II, D-44870 Bochum, Germany
[2] Department of Physics, University of Arizona, Tucson, AZ 85721, USA
[3] Jagiellonian University, Institute of Physics, Reymonta 4, 30-059 Cracow, Poland
[4] Department of Physics, Faculty of Engineering, Kyushu Institute of Technology, 1-1 Sensuicho, Tobata, Kitakyushu 804-8550, Japan
[5] Forschungszentrum Jülich, Institut für Kernphysik (Theorie), D-52425 Jülich, Germany
[6] Karl-Franzens-Universität Graz, Institut für Theoretische Physik, A-8010 Graz, Austria

Received: 1 November 2002 /
Published online: 15 July 2003 –

Abstract. We perform a complete analysis of nd scattering at next-to-next-to-leading order (NNLO) in chiral effective field theory (EFT) and compare our predictions for selected observables with the ones based on conventional nuclear forces.

PACS. 21.30.Cb Nuclear forces in vacuum – 21.45.+v Few-body systems

1 Introduction

Chiral perturbation theory (CHPT) is a powerful tool, which allows to perform model-independent and systematic calculations of low-energy properties of hadronic systems. It is based upon the approximate and spontaneously broken chiral symmetry of QCD. The low-energy hadronic S-matrix elements are obtained via a simultaneous expansion in the low external momenta and quark masses starting from the most general chiral invariant effective Lagrangian for Goldstone bosons (pions in the case of two flavors) and matter fields (nucleons, Δ, ...). If few nucleons are considered, the interaction becomes too strong to be treated perturbatively and an additional resummation of the amplitude is mandatory. According to Weinberg [1], this can be achieved via solving the Lippmann-Schwinger equation with the effective potential derived using the CHPT technique. This scheme has been applied successfully at NNLO to the two-nucleon (2N) system [2–4] and recently to the 3N and 4N systems at NLO [5] and NNLO [6]. The purpose of the present work is to compare our results for nd scattering at NNLO presented in [6] with the ones based on the conventional 2N and 3N forces [7].

2 The chiral 3NF at NNLO

Interactions between nucleons are classified in chiral EFT according to the power of the expansion parameter Q/Λ_χ, where Q is the low-momentum scale and Λ_χ the chiral-symmetry breaking scale of the order of the ρ-meson mass. The pion mass M_π is considered to be of the order Q. For any time-ordered connected diagram contributing to the few-nucleon scattering, which does not contain purely 2N intermediate states, the corresponding power ν of the expansion parameter Q/Λ_χ is given by

$$\nu = -4 + E_n + 2L + \sum_i V_i \Delta_i \,, \tag{1}$$

where E_n, L and V_i are the numbers of external nucleon lines, loops and vertices of type i, respectively. Further, the quantity Δ_i refers to the chiral dimension of a vertex of type i and is defined as

$$\Delta_i = d_i + \frac{1}{2} n_i - 2 \,, \tag{2}$$

with d_i the number of derivatives or M_π insertions and n_i the number of nucleon lines at the vertex i. The inequality $\Delta_i \geq 0$ is valid as a consequence of chiral invariance and is of a crucial importance for the chiral expansion.

We see from eqs. (1), (2) that at LO ($\nu = 0$) the effective Hamiltonian for few nucleons gets only contributions from the 2N interactions given by the tree diagrams with all vertices of dimension $\Delta_i = 0$. At NLO ($\nu = 2$) additional 2N diagrams appear with either $L = 1$ and all vertices of the lowest dimension $\Delta_i = 0$ or with $L = 0$ and one vertex of dimension $\Delta_i = 2$ [1]. Note that the 3NF

[a] e-mail: evgeni.epelbaum@tp2.ruhr-uni-bochum.de

[1] There are no vertices of dimension $\Delta_i = 1$, which would contribute to the tree 2N diagrams.

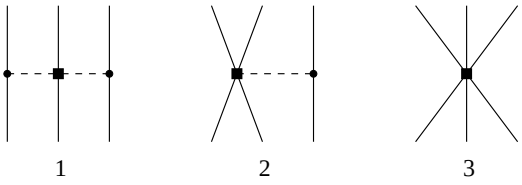

Fig. 1. Three-nucleon force at NNLO. Solid and dashed lines are nucleons and pions, respectively. Heavy dots (solid rectangles) denote vertices with $\Delta_i = 0$ ($\Delta_i = 1$).

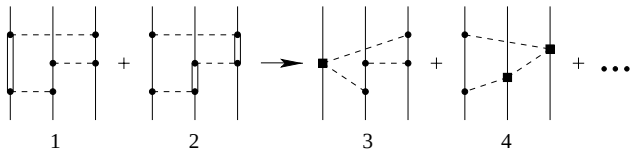

Fig. 2. Three-pion exchange 3NF with one Δ in intermediate states (graphs 1 and 2) and the corresponding 3NF in chiral EFT without explicit Δ's (graphs 3 and 4). Double solid lines represent the Δ-isobar.

would appear at NLO as well, given by the tree diagrams with all vertices with $\Delta_i = 0$. It however turns out that the total contribution of the 3NF at NLO vanishes completely [1,8,3]. The 2N corrections at NNLO result from the subleading (*i.e.* with one πNN vertex of dimension $\Delta_i = 1$) two-pion exchange (2PE) diagrams. The explicit expressions for the 2NF at NNLO are presented in an energy-dependent formulation in [2] and in the energy-independent one in [9,3,4]. A complete NNLO analysis of the 2N system has been carried out in [2,4,10]. The chiral 3NF at NNLO has been worked out in [8]. It is given by the (subleading) 2PE contribution, one-pion exchange (1PE) with the pion emitted (or absorbed) by the 2N contact interaction and 3N contact interaction, see fig. 1. The Pauli principle and the usual symmetry requirements (parity invariance, rotational invariants, ...) lead to a strong reduction of the number of independent terms in the 3NF at NNLO, leaving just one 1PE and one contact operator [6].

It has been demonstrated in [11] that the chiral 2PE 3NF matches with the low-momentum expansion of various existing phenomenological 3NFs provided they respect chiral symmetry. The remaining 1PE and contact contributions are usually not included in the conventional 3NFs. Let us now comment on the recent Illinois models [12], which include, apart from the terms already present in the Urbana IX model [13], a lot of new spin and isospin structures. In particular, the P-wave 2PE 3NF has been taken into account as well as the terms related to the first two diagrams in fig. 2. It is now interesting to see at which order in chiral EFT one would expect contributions from the three-pion exchange (3PE), graphs 1 and 2. In fact, the Δ-isobar plays a special role in chiral EFT due to the small value of the ΔN mass splitting $m_\Delta - m_N = 293$ MeV, which is only twice as large as M_π. For that reason it is not clear *a priori* whether in EFT one should include it explicitly, assuming $m_\Delta - m_\mathrm{N} = \mathcal{O}(M_\pi)$, or integrate it out. On the one hand, inclusion of Δ yields a scheme, which is not strictly rooted in QCD because of the decoupling theorem [14]. On the other hand, it might be a useful phenomenological extension of the chiral EFT and a systematic power counting has already been worked out [15]. Both formalisms are used in the literature. In our approach without explicit Δ's, the leading contributions from the graphs 1, 2 in fig. 2 are represented by the diagrams 3 and 4. Note that the leading $\pi\pi$NN vertices resulting from integrating out the Δ degree of freedom have a dimension $\Delta_i = 1$, while the πNΔ vertices start with $\Delta_i = 0$. Then, according to eqs. (1), (2), graphs 3 and 4 contribute at orders $\nu = 5$ and $\nu = 6$, respectively, *i.e.* are suppressed by 2 and 3 orders of the expansion parameter relative to the leading 3NF shown in fig. 1. If Δ's are included explicitly, the leading 3NF related to the 2PE with an intermediate Δ is shifted one order lower and appears already at NLO with $\nu = 2$. Both graphs 1 and 2 in fig. 2 are then of the same order and contribute at N^{3}LO with $\nu = 4$. Note, however, that additional 3PE diagrams with 2 and 3 Δ's in intermediate states contribute at the same order $\nu = 4$.

3 Results

In [6] we presented the NNLO analysis of the 3N and 4N systems and reported a significant improvement in the description of various observables compared to the NLO calculation [5]. The two unknown parameters in the chiral 3NF have been fixed from the triton binding energy and *nd* doublet scattering length, which allowed us to make parameter-free predictions for various scattering observables. Specifically, we discussed the differential cross-section, vector and tensor analysing powers for elastic *nd* scattering at 3, 10 and 65 MeV as well as the cross-section and vector analysing power for selected deuteron breakup configurations. It is now interesting to compare our results with the ones based upon the conventional NN interactions. The latter have been presented in [7] for elastic scattering (at 3, 65 and higher energies) and in [16] for the breakup. In general, both approaches lead to very similar results up to $E_\mathrm{lab} = 65$ MeV and mostly agree with the data. In what follows, we will only show selected cases, for which different results are observed. We did not find any singificant differences at 3 MeV. At 65 MeV, deviations become more visible. We have also checked that the corrections due to isospin-violating effects not yet included in the chiral analysis are small at that energy, so that a direct comparison with the results of [7,16] is possible. In fig. 3 the tensor analysing powers T_{20}, T_{21} and T_{22} for elastic *nd* scattering are shown. The uncertainty of the chiral predictions refer to the cut-off variation in the range from 500 to 600 MeV. The light-shaded band results from taking the AV18, CD Bonn, Nijm I, II and 93 NN forces together with the Tucson Melbourne (TM) 3NF [17]. The cut-off parameter in the conventional 3NFs is always adjusted in the way to reproduce the triton binding energy. Note that the TM 3NF violates chiral symmetry [11]. The TM$'$ 3NF refers to the chiral invariant 3NF based upon

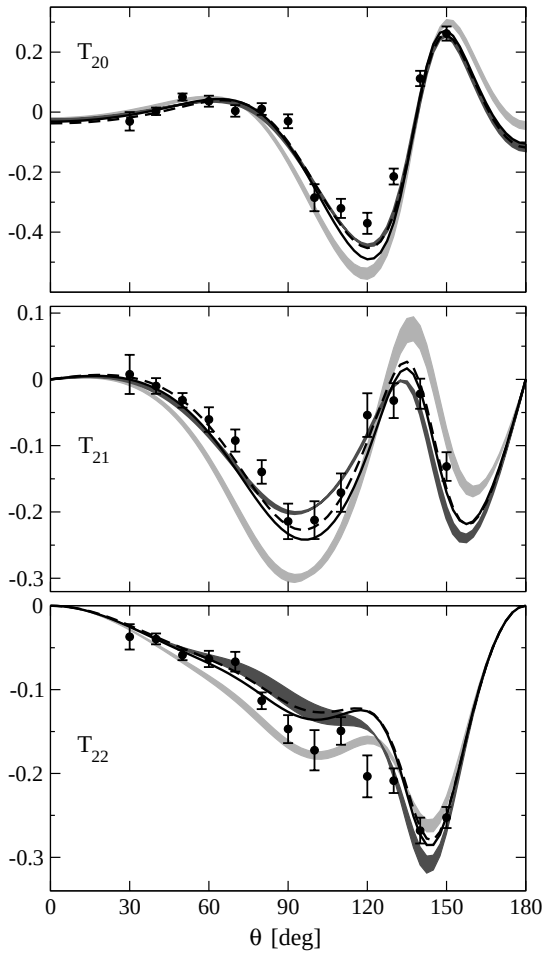

Fig. 3. *nd* tensor analysing powers T_{20}, T_{21} and T_{22} at 65 MeV at NNLO in chiral EFT (dark-shaded bands) compared to the conventional NN forces + TM 3NF predictions (light-shaded bands) and to the *pd* data from [18]. The solid (dashed) lines refer to the AV18 + URBANA IX (CD Bonn + TM′) results.

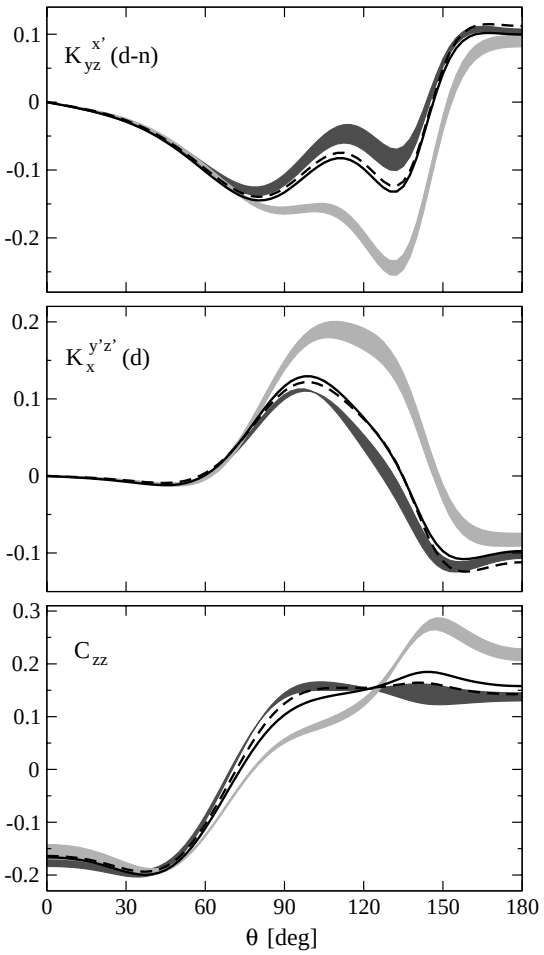

Fig. 4. The spin transfer coefficients $K_{yz}^{x'}$, $K_{x}^{y'z'}$ and C_{zz} for elastic *nd* scattering. Curves as in fig. 3.

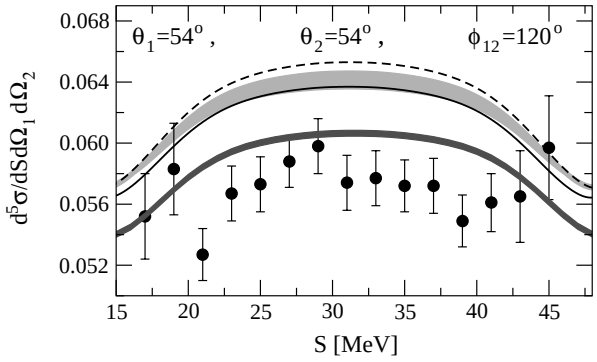

Fig. 5. *pd* breakup cross-section data (in mb MeV^{-1} sr^{-2}) along the kinematical locus S (in MeV) at 65 MeV. *pd* data are from [19]. Curves as in fig. 3.

the TM 3NF. It is remarkable that the largest deviations are observed for the TM 3NF, which violates chiral symmetry. Chiral predictions are rather close to both, the AV18 + URBANA IX and CD Bonn + TM′ ones, which all show a better agreement with the data than the TM results. Note that there might be additional corrections due to the Coulomb force, which are not taken into account. The situation with the theoretical predictions of the spin transfer coefficients shown in fig. 4 is qualitatively very similar. The largest deviations appear again for the TM 3NF. Unfortunately, no data are available for these observables.

We also show in fig. 5 the differential cross-section in the specific breakup configuration, for which the largest deviations between the two approaches are observed.

4 Summary

We observe, in general, a good agreement between chiral predictions at NNLO and results based upon conventional 2N and 3N forces and with the data for *nd* scattering at energies below 65 MeV. Largest deviations occur for the TM 3NF, which violates chiral symmetry. More data of high quality are needed to test the chiral EFT in the 3N system and to probe the spin structure of the 3NF.

References

1. S. Weinberg, Nucl. Phys. B **363**, 3 (1991).
2. C. Ordóñez *et al.*, Phys. Rev. C **53**, 2086 (1996).
3. E. Epelbaoum *et al.*, Nucl. Phys. A **637**, 107 (1998).
4. E. Epelbaum *et al.*, Nucl. Phys. A **671**, 295 (2000).
5. E. Epelbaum *et al.*, Phys. Rev. Lett. **86**, 4787 (2001).
6. E. Epelbaum *et al.*, arXiv:nucl-th/0208023.
7. H. Witała *et al.*, Phys. Rev. C **63**, 024007 (2001).
8. U. van Kolck, Phys. Rev. C **49**, 2932 (1994).
9. N. Kaiser *et al.*, Nucl. Phys. A **625**, 758 (1997).
10. E. Epelbaum *et al.*, Eur. Phys. J. A **15**, 543 (2002), arXiv:nucl-th/0201064.
11. J.L. Friar *et al.*, Phys. Rev. C **59**, 53 (1999).
12. S.C. Pieper *et al.*, Phys. Rev. C **64**, 014001 (2001).
13. B.S. Pudliner *et al.*, Phys. Rev. Lett. **74**, 4396 (1995).
14. J. Gasser, A. Zapeda, Nucl. Phys. B **174**, 445 (1980).
15. T.R. Hemmert *et al.*, J. Phys. G **24**, 1831 (1998).
16. J. Kurós-Żołnierczuk *et al.*, arXiv:nucl-th/0203020.
17. S.A. Coon, W. Glöckle, Phys. Rev. C **23**, 1970 (1981).
18. H. Witała *et al.*, Few-Body Syst. **15**, 67 (1993).
19. J. Zejma *et al.*, Phys. Rev. C **55**, 42 (1997).